BNL-65672
ATD/APT94-0004 (Rev. 1)

CALORIMETRIC MEASUREMENT OF AFTERHEAT IN TARGET MATERIALS FOR THE ACCELERATOR PRODUCTION OF TRITIUM

By

R. B. Perry
Argonne National Laboratory
Electronics Technologies Department
Electronics and Computing Technologies Division

and

M. S. Zucker
Brookhaven National Laboratory
Department of Advanced Technology
Applied Technology Division

June 1, 1994

DISCLAIMER

BNL-65672

Calorimetric Measurement of Afterheat in Target Materials for the Accelerator Production of Tritium*

By:

R.B. Perry
Argonne National Laboratory
Electronics and Computing Technologies Division

and

M.S. Zucker
Brookhaven National Laboratory
Department of Advanced Technology

* This work was performed under the auspices of the U.S. Department of Energy. The manuscript has been authored by a Contractor (grantee) of the U.S. Government under Contract No. DEAC0298CH10886.

CALORIMETRIC MEASUREMENT OF AFTERHEAT IN TARGET MATERIALS FOR THE ACCELERATOR PRODUCTION OF TRITIUM

I. INTRODUCTION

The estimate of afterheat in a spallation target of lead (Pb) or tungsten (W), by calorimetry, is the purpose of this experiment in support of the Accelerator Production of Tritium (APT). Such measurements are needed to confirm code calculations, these being the only practical way of gaining this type of information in a form suitable to aid the design of the APT machine. Knowledge of the magnitude and duration of afterheat resulting from decay of activation products produced by proton bombardment of the target is necessary to quantify APT safety assumptions, to design target cooling and safety systems, and to reduce technical risk.

Direct calorimetric measurement of the afterheat for the appropriate incident proton energies is more reliable than the available alternative, which is indirect, based on data from gamma-ray spectroscopy measurements. The complex x-ray and gamma-ray spectra from an irradiated Pb sample, shown in Figure 1, contains more than 400 resolvable peaks. Matching this number of peaks to known spectra, in order to deduce individual isotopes and their decay chains, as is required to determine the afterheat in this manner, is difficult, involves uncertainties, and is very time consuming. In contrast, direct determination of afterheat using calorimetry is much more straightforward, although it involves some knowledge of the gamma spectral energy distribution to make a correction as will be discussed below. This will be illustrated with the results obtained from direct calorimetric assay of irradiated Pb and W samples.

The Brookhaven Linac Isotope Producer (BLIP) was chosen as the irradiation facility for testing calorimetry as an afterheat measurement technique because a hot-cell facility is contiguous and integrated with the BLIP target irradiation area, allowing measurements to be made safely and relatively quickly without requiring extensive modification or augmentation of existing equipment.

The afterheat deposited at a depth into the target will depend on the proton energy at that depth, and therefore these measurements should be made over the whole range of energies, i.e., up to and including 1.0 GeV, the present design goal of the APT (LINAC) accelerator. The BLIP beam-line is limited to 0.2 GeV, and so the present reported results are for this incident energy only. (Allowing for the loss of energy as the protons traverse these samples, the actual energies of the protons are estimated to be in the range 0.182 ± 0.018 and 0.167 ± 0.033 GeV for the Pb and W samples respectively.) Plans to extend these measurements to as much as 1.5 GeV will be discussed later in this report.

The Small Sample Calorimeter (SSC) used for these measurements was originally developed by Argonne National Laboratory (ANL), and was intended for measuring heat from alpha decay in long-half-life isotopes of plutonium. Though not required for its originally intended application, this calorimeter had one feature in particular that suited it uniquely to the present

application, namely, the ability to respond to transient heat production on a time scale suitable to assay afterheat induced by proton bombardment. The afterheat created in the Pb and W samples by the BLIP beam was also in the appropriate range (10 to 50 mW) for this calorimeter, so that the irradiation times required were convenient. However there were modifications made to the calorimeter to improve assay of short-half-life isotopes decaying by beta and gamma-ray emission:

1. Replacement of the sample chamber plug with a sliding cover for easy operation with remote-handling manipulators in a hot-cell environment.

2. Elimination of the preheating step (to improve the rapidity with which samples can be inserted and removed) by increasing the power available for (more) internal preheating.

3. Modification of the data-acquisition software to increase the sampling rate of the analog-to-digital converter (ADC), which improves the precision by providing more data points for the curve-fitting program.

4. Replacement of the aluminum sample chamber liner with a tungsten liner to improve the absorption of gamma rays and aid in the evaluation of the gamma contribution to the afterheat.

These modifications were made by the ANL Electronics and Computing Technologies Division (ECTD). Afterheat measurements were made with the modified ANL Small Sample Calorimeter on Pb and W samples irradiated at BLIP during July 21-23, 1993. (The initial trial of this measurement system before these improvements were made was in August 1992. Other relevant information about the calorimeter are given in the following).

II. CALIBRATION

The modified SSC was tested and calibrated at ANL against electrical standards. The calorimeter was calibrated with an electrically heated sample capsule following the procedure documented in the SSC operating manual [1]. The required voltage measurements were made with a recently calibrated, 5½ digit, digital volt meter (DVM). (The DVM calibration is traceable to NIST standards verifiable through ANL Electronics and Computing Technologies Division's CS4 Documentation.) A diagram of the calibration test set-up, from the instrument's manual, is shown in Figure 2.

III. MEASUREMENT PROCEDURE

Each sample was contained in an aluminum capsule with a gas-tight electron-beam-welded cover.

(Electron-beam welding ensures containment integrity, but requires a vacuum, leaving the capsules evacuated after welding.) The capsules were held in a jig or "coupon", which was a thin aluminum plate with a clip to hold the capsule that allowed reproducible positioning with respect to the proton beam. This was moved to the BLIP target position and irradiated underwater at an ambient water temperature of 20°C. The jig originally had been designed to correct for an earlier misalignment of the beam. In this experiment the beam axis had a new position, which unfortunately put the sample capsule distinctly off center. However, the actual fluence of protons through the sample was monitored using an aluminum activation monitor foil wrapped around the capsule so that there was a one-to-one correspondence between fluence through the monitor foil and the sample. The heat induced by proton bombardment was conducted to the water through the tightly fitting aluminum capsule. The samples were then conveyed from the irradiation facility to the adjoining hot-cell using a remote-controlled chain-drive mechanism. All subsequent operations used remote manipulators, as the samples were dangerously radioactive after irradiation. The capsules were dried and punctured (to admit air to improve heat transfer during the calorimetry), and inserted into the calorimeter.

The SSC is an isothermal, heat-flow, calorimeter. It measures the power from a sample decaying in heat power output by monitoring the additional power supplied to the sample chamber by a closed-loop temperature controller which endeavors to keep the chamber temperature constant, in this application, at 45 °C, as the power from the sample in the chamber changes. As the sample afterheat power decays, this decrease is compensated for by an increase in the electrical heating power from the instrument, trying to maintain the set temperature constant. The samples introduced into the calorimeter in the present experiment were always below this set temperature, as indicated by the immediate full-power ("saturation") responses of the controller when each of the samples was inserted. Samples that were at a higher temperature than the chamber set-point would have driven the controller to decrease or even cut off all power. An unirradiated-sample time-dependent power input curve is used to establish the baseline response. The power from afterheat is represented by the difference between that baseline and the power-input time dependence of the irradiated sample. Calorimeter response curves for an unirradiated lead sample are shown in Figure 3, which illustrates a typical measurement sequence.

Insertion of a room-temperature, unirradiated, sample cools the measurement chamber below its set point, causing the control system to respond with full heating power until the temperature of this unirradiated sample rose to the operating temperature of the calorimeter. The data for this curve is composed of the average power for consecutive 10-second intervals during each one of which power measurements were made at 1 second intervals. The time delay (approximately 120 seconds) indicated by the flat response before the sharp rise in power shown in Figure 3 (dashed line) represents the time (after the beam was shut off, "EOB") required to bring the sample into the hot cell, dry and puncture the capsule, and insert it into the calorimeter. The delay time was simulated in the baseline measurement (solid line) by delaying insertion of the sample for several minutes after the data acquisition was started. No useful data are obtained while the power delivered by the control electronics is at its maximum possible value

(saturation). The unirradiated sample produces no heat, so the power produced by the controller promptly returns to the baseline after the temperature of this sample reaches the set temperature.

Initially the irradiated sample causes a similar response as shown by the dashed line in Figure 3. However in this case, after the sample is heated to the calorimeter temperature, the self-heating due to radioactive decay acts to raise the sample temperature further, causing the control system to reduce the electrical power in order to maintain the control temperature. The difference in control power in the two cases is the power produced by radioactive decay of the sample.

Power-difference measurements are made by time shifting the points, and matching the first point at which the calorimeter supplies less than the maximum power output to the unirradiated sample, with the first such point on the irradiated sample curve. Power measurements were started at the end of beam (EOB), before sample insertion, to provide an accurate time mark so that the fitted response curve could be extrapolated back to the EOB. The first 10-15 data points are collected with no sample in the calorimeter, and represent the baseline power of the calorimeter. These points are compared to the first points in the unirradiated curve to correct for any baseline drift. The procedure for extracting the afterheat power from the calorimeter response is as follows:

1. Correct for baseline drift by subtracting the difference between starting power before the sample is inserted and the baseline before insertion of the unirradiated sample.

2. Correct for any time difference by shifting the time scale of the data from the unirradiated sample to coincide with time scale of the data from the irradiated sample using the first unsaturated points of each as the reference point.

3. Subtract the baseline-adjusted irradiated-sample data from the unirradiated-sample data, point by point.

An additional 50 to 60 seconds is required for the control system to settle down before the data starts to follow a smooth monotonic curve typical of decay of a radioactive source with no significant buildup of daughter products, at least as regards heat production. This smooth decay curve started 500-550 seconds after EOB. Power difference curves for Pb samples are shown in Figure 4.

Sample irradiation at BLIP is computer controlled. The beam current is continuously monitored by a current integrator and the beam is shut off when the prescribed quantity of charge has been delivered to the target area. This area is somewhat larger than the projected frontal area of the sample, and so the actual proton fluence through the sample was determined by the ^{24}Na activation of an Al foil wrapped around each sample capsule, the current integrator value just furnishing a convenient way of approximately normalizing the irradiation times. The actual irradiation time, i.e., Start-of Beam minus End-of-Beam (SOB - EOB) was noted for each irradiation. The current integrator unit of charge is one peculiar to accelerator isotope

production facilities, the "μAmpere · hour" (μAh), representing the charge of 2.25×10^{16} protons.

Each sample run involved several operations for which there could be difficulties that might mar the measurement to a greater or lesser extent, and unfortunately, such mishaps were the rule, not the exception, as the experimental techniques were new to the personnel involved. Future improvements to the experimental system as a whole would greatly alleviate or totally obviate these difficulties, as will be discussed later in this report. However there were two unflawed runs, one each for Pb and for W. Each one serves to define the capability of the measurement system in the assay of afterheat induced by proton bombardment. The following is a selection of the Pb results illustrating some of the things that went wrong in the present series of irradiations, along with that one Pb irradiation (sample 002) in which all the segments of the measurement process appeared to work flawlessly.

Sample 000 was irradiated for 3 μAh (6.75×10^{16} total protons) as a test to determine the proton dose needed to produce samples with power in the measurement range of the calorimeter; more irradiation would have made better use of the available range of the instrument. Based on this result, the remaining lead samples shown in Figure 4 were irradiated for 10 μAh (2.25×10^{17} protons) to provide a higher sample activity. Measurements were made for 1500 seconds after the beam was turned off, at 1-second intervals, with every 10 consecutive measurements averaged to yield a total of 150 data points representing the decay curve. The differences in amplitude and shape shown in the four curves in Figure 4 are discussed below:

0. Pb sample 000 was a 3 μAh test irradiation to determine the dose needed for optimum activity. No dosimetry foil was included with the sample so that the otherwise flawless run could not be used.

1. Pb sample 002 - After the perturbation caused by inserting a cold sample into the calorimeter dies away, the curve has a shape that cannot be fit with a single exponential as would be expected for a sample containing several radioactive nuclides; this is the unflawed Pb result.

2. Pb sample 005 - The second rise in the power indicates that the capsule was not properly dried before it was punctured, and some water was drawn into it. The fact that heat was used to evaporate this water during the early part of the measurement spoiled assay of the short term component of the afterheat.

3. Pb sample 012 - The flat region at the start of the decay curve that is caused by the calorimeter power being driven to cut off, caused by the sample power exceeding the measurement range of the calorimeter due to over irradiation.

IV. DATA ANALYSIS

The computer software entitled "SigmaPlot Ver. 5.01" (Jandel Scientific) was used to process

the data, plot the curves, and fit a sum of decaying exponentials to the declining portion of the curve. The SigmaPlot fitting routine uses the Marquardt-Levenberg algorithm. A semilog plot using a natural-log scale for the power, as in Figure 5, shows that all samples are decaying with the same final time constant. The plot of the logarithm of the decay power for the last 500 seconds of data against time is linear showing that the measurement points in this region are adequately fit by a single decaying exponential. As is often the case, greater precision was obtained with the fitting routine by first fitting a single exponential to the tail of the curve and thus determining the longer time constant. This value was then entered as a constraint in the double-exponential fit to Equation 1. A double-exponential model fits the data very well for times after that time when the calorimeter recovers from insertion of a sample cooler than the calorimeter temperature, as shown in figure 6 for the total power as a sum of two decaying exponentials,

$$P = P_1 e^{-\lambda_1 t} + P_2 e^{-\lambda_2 t} \tag{1}$$

The total heat that would be emitted by the sample from the end of irradiation on can be calculated from the time integral of equation (1), giving the result shown in equation (2).

$$\begin{aligned} Q &= P_1 \int_0^\infty e^{-\lambda_1 t} dt + P_2 \int_0^\infty e^{-\lambda_2 t} dt \\ &= \frac{P_1}{\lambda_1} + \frac{P_2}{\lambda_2} \end{aligned} \tag{2}$$

When P is in milliwatts and λ is in sec^{-1}, then the total amount of afterheat "Q" will be in millijoules. The variance of "Q" is given

$$V(Q) = \left(\left(\frac{1}{\lambda_1}\right)^2 (s(P_1))^2 + \left(\frac{1}{\lambda_2}\right)^2 (s(P_2))^2 + \left(\frac{P_1}{\lambda_1^2}\right)^2 (s(\lambda_1))^2 + \left(\frac{P_2}{\lambda_2^2}\right)^2 (s(\lambda_2))^2\right. \tag{3}$$

by equation 3 where s(P) and s(λ)are the uncertainties in the values.

V. LEAD SAMPLES

Lead samples prepared for this measurement series were hollow cylinders weighing 23 grams compared to 28 grams for a solid cylinder. Sample weight was reduced by boring out the

center, rather than reducing the overall sample diameter, in order to maintain a close fit with the sample capsule for good heat transfer. The intent was to reduce the preheating time by reducing sample mass in order to start data collection a little closer to EOB. However, the improvement was small because of the relatively large heat capacity of the aluminum capsule. This was not a limiting factor in the experiment.

For the reasons stated earlier, only one of the measurements made on Pb seemed satisfactory in all ways and is therefore the one used to extract the quoted results.

Figure 6 shows the calorimeter response for Pb sample 002 with baseline subtracted and the fitted curve extrapolated back to the end of beam. This measurement was terminated after 1500 seconds. Short-time-constant and long-time-constant components of the fitted curve are also shown as EXP-1 and EXP-2. Curve-fitting results are shown in Table I. Integration of the curve given in equation (2) over all time gives the total heat output "Q". The uncertainty s(Q) is given by the square root of the variance calculated from equation (3) using the uncertainties in the fitting parameters. The fitting uncertainty include the random uncertainty in the calorimeter measurements.

The double-exponential model fits the experimental data very well over the measurement period of 1500 seconds for the Pb samples. However, this does not necessarily indicate that only 2 isotopes are the primary heat sources. There may be many isotopes contributing significantly to the afterheat even at 0.1 GeV, and the "two-exponential model" may simply represent a convenient way of summarizing two collections of time constants, one centered about a comparatively shorter value, the other clumped about the longer value. (It is often the experience in fitting exponentials to data in which several decays are close together in their respective time constants, that the fitting procedure will lump these together, giving a single result having a time constant that is some sort of average.) There are about 31 radioactive Pb isotopes with lower atomic weight than the 4 naturally occurring Pb isotopes, and their halflives range from 0.6 sec to 5.3×10^4 years. Of these, there are 12 Pb isotopes with halflives in the range of 1-43 minutes. Modes of decay include positron emission, electron capture, isomeric transition, and alpha emission. Isotopes with lower atomic number could also be produced by proton irradiation at 0.2 GeV. Thus, there is no shortage of possible suspects! There is interest in determining just which nuclides are contributing to the decay heat, but determining their identities is not necessary to satisfy our requirements. The only things needed for engineering and safety considerations are the total afterheat, and the time behavior of the total afterheat power. In fact, an important justification for this work is just that this method allows determination of the afterheat without going into laborious preliminary determinations of decay schemes, nuclide production quantities, etc..

Table I results from the curve-fitting routine and application of equations 1, 2, and 3.

TABLE I. SUMMARY OF CURVE-FITTING RESULTS FOR LEAD AND TUNGSTEN

23-GRAM LEAD SAMPLE AND 48-GRAM TUNGSTEN SAMPLE IRRADIATED AT BLIP 7/93 WITH 200-MEV PROTONS

SAMPLE	$P_1(10^{-16}mW/g*p)$	$s(P_1)$ (10^{-16})	$\lambda_1(1/SEC)$	$s(\lambda_1)$	$P_2(10^{-16}mW/g*p)$	$s(P_2)$ (10^{-16})	$\lambda_2(1/SEC)$	$s(\lambda_2)$	$Q(10^{-16}J/g*p)$	$s(Q)$ (10^{-16})
Pb S.00 2	1.726	±0.021	0.000407	±0.000005	5.34	±0.54	0.0061	±0.0002	5.12	±0.12
W S.007	2.051	±0.005	0.000410	±0.000004	5.10	±0.04	0.00254	±0.00003	7.01	±0.06

VI. TUNGSTEN SAMPLES

The W samples, are 48-g solid cylinders of pure tungsten metal cut to length from barstock and ground to size. No attempt was made to reduce the weight of the W samples by drilling out the axial part because the difficulty of machining tungsten didn't seem worth the result. Irradiation for 3 μAh proved to be adequate for the W samples. These samples were encapsulated and handled in the same manner as the Pb samples. Calorimetric data with baseline subtracted are shown in Figure 7 for the 4 samples that were irradiated. Problems similar to those encountered with the Pb samples are indicated by examination of the curves in Figure 7. The best data are those obtained with sample 007 as noted below:

1. W sample 003 - There were delays encountered in the handling of this sample which resulted in an unacceptably long time before the start of the calorimetry.

2. W sample 006 - The curve indicates that the capsule was not dried thoroughly before puncturing.

3. W sample 007 - After the perturbation caused by inserting a sample (distinctly cooler than the temperature set point) into the calorimeter dies away, the curve has a "sum of decaying exponentials shape" that would be expected for a sample containing several radioactive nuclides.

4. W sample 010 - The sample was slightly over-irradiated and thus the power output was initially above the measurement range of the calorimeter, causing a delay in the start of the exponential decay curve.

The measurement time was extended to 2500 seconds (250 data points) for W samples 006, 007, and 010. It was found that extending the measurement time significantly reduced the error in the parameters determined by fitting. Ruling out consideration of all W measurements known to be flawed in some way, left only one W measurement, 007.

The double-exponential model fits the experimental data very well as shown in the plot of sample 007 in Figure 8, but as is the case with Pb, there are many isotopes that conceivably could contribute to the decay heat; listed half-lives range from 0.08 sec to 121 days; there are seven tungsten isotopes with halflives in the range 1.65 to 37.5 minutes. The average energy of the gamma rays emitted are less than 0.4 MeV. The maximum energy is 0.835 MeV but the higher-energy gamma rays are relatively improbable. Therefore most of the gamma-ray energy will be absorbed in the sample or in the tungsten liner of the calorimeter, as will be discussed below.

VII. DISCUSSION OF AFTERHEAT EXPERIMENT RESULTS

The afterheat per incident proton is calculated from dosimetry data obtained from the aluminum foil flux monitor. The total proton fluence to sample 002, based on foil activation calculations, was 1.18×10^{16} protons (5% of the available protons) for a 10 μAh irradiation. A sample irradiated in a similar experiment in 1992 had a total fluence of 1.61×10^{16} protons (24% of the available protons) for a 3-μAh irradiation. This is an objective estimate of the degree that samples were not centered in the beam during the 1993 experiments. (We were informed, at a time too late for us to do anything about it, that the position of the beam with respect to the target coupon had changed.) The heat/(gram·proton) for these (Pb) samples is given below:

1992 Sample #15: Afterheat = 1.9×10^{-16} J/g•p.

1993 Sample.002: Afterheat = 5.1×10^{-16} J/g•p.

The ratio of the results is 2.7. The increase in measured heat is believed to be due to absorption of gamma-ray energy in the tungsten liner installed for that purpose.

The best results, based on fitting error and observation of curve shape, were obtained for Pb sample 002 and W sample 007. The afterheat per gram·proton taken from Table I is:

Pb $(5.1 \pm 0.12) \times 10^{-16}$ J/g•p

W $(7.0 \pm 0.06) \times 10^{-16}$ J/g•p

These calorimetry results indicate that a tungsten target of equal mass irradiated for a short time (i.e., not to saturation), may produce 1.4 times as much afterheat as a lead target when irradiated with the same fluence of 200-MeV protons.

VIII. GAMMA-RAY HEATING

The efficiency of the calorimeter for measuring gamma-ray heating depends on the energy and abundance of the gamma rays emitted by the sample. Calculations of the self-absorption of Pb or W samples and of external absorption in the W liner of the calorimeter are discussed below:

Self-absorption:

The self-absorption of gamma-ray radiation in a cylindrical source can be calculated from the following expression taken from "On the Calculation of the Self-Absorption in Spherical Radioactive Sources" Nuclear Instruments and Methods, Vol. 117, (1974):

$$\frac{J}{J_o} = \frac{\Gamma(p+1)}{(\mu R)^p} [I_p(2\mu R) - L_p(2\mu R)] , \qquad (4)$$

where p=1 for a cylinder, $I_p(2\mu R)$ is the modified Bessel function, and $L_p(2\mu R)$ is the modified Struve function. The gamma function $\Gamma(2)=1$. The equation can be rewritten for the cylinder:

$$\frac{J}{J_o} = \frac{1}{\mu R} [I_o(2\mu R) - L_o(2\mu R)] 1. \qquad (5)$$

The value of R is 0.737 cm for the Pb or W samples used for the afterheat measurements by calorimetry. Values of J/J_o (transmitted radiation divided by the emitted radiation) are shown in Table II for gamma-ray energies up to 2.5 MeV. (Pb isotopes do produce gamma rays of up to that energy.)

I/I_o (transmitted divided by the incident radiation) in Table II represents the absorption of gamma rays in the W liner of the calorimeter. Gamma rays with energy less than 0.3 MeV will be fully absorbed in the sample and calorimeter. The absorption in the tungsten liner will be somewhat greater than shown because the calculation does not take into consideration gamma rays passing through the wall obliquely. However, the lead cylinder was not solid so that J/J_o somewhat over estimates.

TABLE II. GAMMA-RAY ABSORPTION IN LEAD SAMPLES

Energy MeV	$\mu(cm^{-1})$	μR	J/J_o	I/I_o	Total
2.5	0.48	0.35	0.754	0.811	0.61
2.0	0.5	0.37	0.743	0.802	0.60
1.5	0.58	0.43	0.709	0.776	0.55
1.0	0.78	0.58	0.638	0.720	0.46
0.5	1.6	1.18	0.442	0.462	0.20
0.3	3.1	2.28	0.260	0.232	0.06

A similar calculation can be made for the W samples as shown in Table III.

TABLE III. GAMMA-RAY ABSORPTION IN TUNGSTEN SAMPLES

Energy MeV	$\mu(cm^{-1})$	μR	J/J_o	I/I_o	Total
1.0	1.24	0.914	0.511	0.720	0.37
0.75	1.65	1.216	0.429	0.646	0.28
0.5	2.91	2.145	0.278	0.462	0.13

Values of gamma-ray self-absorption in W could not be calculated for energies lower than 0.5 MeV because the value of $2\mu R$ exceeded the range of tabulated values for the modified Bessel and Struve function.

The above estimation of gamma-ray absorption indicates that while a significant fraction of the lower-energy gamma rays will be absorbed in the wall of the calorimeter sample chamber, there may be higher energies present for which an appreciable fraction of the gamma photons could escape. The amount of energy they represent is expected to be minor, as there is a rapid (approximately) exponential decrease in the intensity (activity) of gamma photons from irradiated material with increasing photon energy. The loss in contribution to the measured afterheat because of gamma rays escaping from the calorimeter could be obtained from a transport-code calculation, accurately enough for the purpose of making a correction to the measured value. These calculations have not been made.

IX. GAMMA-RAY SPECTROSCOPY DATA

For the purpose of making an estimate of the absorption of gamma rays by the calorimeter, in the absence of calculations of the sort mentioned above, some of the results of the activation experiments with Pb and W (at BNL in another experimental phase of the APT program) were made available by Dr. C. Laird of Eastern Kentucky University. A Pb sample irradiated with 1-GeV protons and measured 1.5 hours after irradiation was selected as an example to illustrate the calculation of the fraction of gamma-ray heating that might be missed due to escape of the gamma rays. The gamma-ray spectrum from this sample (3P0001) is the one illustrated in Figure 1. (Measurements within 8 minutes of EOB, matching the time duration of the calorimeter measurements, were not available, and would in fact be quite difficult to obtain because the samples are so intensely radioactive that close to EOB, that a high-resolution gamma detector would probably not be able to function in the intense gamma and X-ray flux. The ability to work closer to the EOB is indeed another advantage for the calorimetric method of measuring afterheat.) A peak-fitting program established the energy and absolute intensity of 392 gamma rays from 0.047 to 1.9 MeV. (These data are still under study at the time this information was conveyed.) A plot of the absolute intensity vs. energy is given in Figure 9. This illustrates the relative abundance of low-energy gamma rays.

The heating effect of the gamma rays depends on the number and energy of gamma rays absorbed. The absolute intensity multiplied by the gamma energy and the fraction that is absorbed is the power in the gamma flux from the sample that is converted to heat in the target. The vertical bars in Figure 9 show the power in microwatts for each gamma-ray line in the spectrum. Data from Table III can be applied to the data in Figure 9 to calculate the fraction of the power available to heat the sample and calorimeter measurement chamber. Figure 9 also shows the result of this calculation superimposed on the total power denoted by the open circles. When these data are summed over the entire spectrum, the result shows that 69% of the available gamma rays for this sample would be measured by the calorimeter. Of course, knowing this number enables inference of the correction factor to be applied to the calorimeter-derived results. The smaller the amount not detected by the calorimeter, the more accurate this correction can be, all other things being equal.

The above calculation is not directly applicable to the calorimeter measurements made at BLIP because of the different proton energy and time after EOB. However, the data will be helpful in designing future experiments.

X. IMPLICATIONS FOR A SPALLATION TARGET

In the following, the experimental data for the Pb and W samples assayed in this experiment that are listed in Tables I and II will be related to the afterheat that would develop in a spallation target of Pb or W at a depth into the target where the proton energy is 200 MeV.

If a particular nuclide with a decay constant λ has a decay heat power output P after the target

has been bombarded by protons at a constant rate for a time t, and the proton irradiation were allowed to proceed indefinitely, the power output would increase to a saturation value

$$P_{\infty} = \frac{P}{1-\exp(-\lambda \cdot t)} . \qquad (6)$$

If the proton bombardment ceases at some time after the target is close to saturation, the total afterheat energy that would develop from that nuclide would be

$$Q = \frac{P_{\infty}}{\lambda} . \qquad (7)$$

The total ("saturation") afterheat output per mass "m" and current density "j" is Q/(m•j), where "m" is the mass of the sample used and "j" is the current density of the beam passing through the sample. Applying these relations to the experimental data and sample parameters gives the results in the following table:

Table IV. SATURATION AFTERHEAT FOR 200 MeV PROTONS.

Input Data	Pb		W	
Sample mass (g)	23		48	
Proton fluence, p, (10^{16})	1.181		0.361	
Irradiation time, t, (s)	915		274	
Sample area (cm^2)	2.161		2.161	
Decay constant, λ, (s^{-1})	4.07×10^{-4}	6.1×10^{-3}	4.1×10^{-4}	2.54×10^{-3}
Power (EOB), P, (10^{-16}mW/g•p)	1.726	5.34	2.051	5.10
Derived quantities:				
Afterheat, Q, (J)	371.9	21.65	807.72	66.29
Tot. aftht. Q_T, (J)	393.60		874.00	
$Q_T/(m \cdot j)$ [10^7J/(g•A/cm^2)]	1.60		1.60	

To illustrate the use of this table, consider the SILC target.

The current per unit area for a 1.4 m x 1.4 m target surface area passing 200 mA of beam is 1.02×10^{-5} A/cm^2. Therefore, at a position inside the target where the beam energy has dropped to 200 MeV, the total heat released by a gram of lead after the end of beam would be $(1.60 \times 10^{7})(1.02 \times 10^{-5}) = 163$ J per gram, to be compared with the heat of fusion for Pb, which is about 23 J per gram. (This calculation assumed for simplicity no loss of protons from the beam as it penetrates the target.) To the extent that the present experiment may under estimate the afterheat by not capturing all of the gamma photons, estimated to be about 30%, the above estimate would have to be augmented by that amount. (With more confidence in that calculation, the correction could be incorporated into the quoted value. For the present, we will confine the quoted values to what was actually measured.)

Note that for irradiations over a long enough time that saturation is achieved, the decay heat on a per unit mass basis seems to be the same for Pb and W, though (as mentioned above) for short irradiations, the afterheat for W would be greater than for Pb.

X. CONCLUSIONS

The basic concept, a direct measurement of decay afterheat which bypasses the laborious classical way of determining this quantity, has been demonstrated to work.

The gamma-ray energy given off by the decay products produced in the activation of lead or tungsten with high-energy protons apparently does represent a significant fraction of the total decay energy. A calorimeter designed for measurement of isotopes decaying by alpha emission must be modified to reduce energy lost with escaping gamma rays. Replacement of the aluminum liner with a tungsten liner in the SSC measurement chamber resulted in a 270% increase in measured heat, proving that the energy loss in the earlier (1992) measurements was significant. Gamma-ray measurements are needed to confirm the gamma-ray absorption calculations for the calorimeter to determine the correction for loss of heat due to transmission of high-energy gamma rays through the calorimeter walls.

The experiments at BLIP have shown that calorimetry can be a useful tool in measuring the afterheat in APT target materials. Gamma-ray spectroscopy measurements on foils irradiated simultaneously with the calorimetry samples would facilitate calculation of the efficiency of the calorimeter for measuring gamma-ray heating of the sample.

XI. FUTURE PLANS

Irradiation of APT target samples at energies between 0.3 and 1.0 or 1.5 GeV for calorimetric measurements is an excellent candidate for follow on work. As indicated earlier in this report, the evaluation of afterheat production at intermediate energies up to the actual bombardment energy of the accelerator is required to characterize fully the afterheat in a target. This future work would make use of the BNL Booster accelerator. This accelerator has several features that

are favorable to this application. Besides the beam energy being variable over the required range, the beam spot intensity is of the correct order of magnitude for the APT concept, the beam current can be measured with an uncertainty approaching as little as 1%, and is finely focussed (compared to BLIP), allowing for smaller samples and more precise geometric control and irradiations coming closer to saturation. Use of the Booster will require a "rabbit" system for transferring the samples from the beam line to the calorimeter. This brings with it a distinct advantage, which would greatly increase the ability to assay samples closer to the EOB, and remove the present requirement for "hands on" remote manipulators. The calorimeter measurement chamber would be restructured for this type operation. An open tube type configuration in a horizontal position similar to that in an existing calorimeter developed for 15-cm-long fuel pins is being considered. In a rabbit system for sample transport, cooling of the sample during and immediately after irradiation to just below the chamber set temperature would be effected using air (or another gas) for cooling, which would do away with the problems caused by water cooling. Since the Booster beam is much more finely focused, samples could be smaller and be irradiated for longer times; the calorimeter would have to be reconfigured for the smaller samples, but this is desirable anyway, as well as the rabbit loading and unloading of the calorimeter. The present limitation on how close assay can be to the EOB is due to the slow transport device (a chain-drive) and the necessity for use of remote hand manipulators to handle the samples and load the calorimeter. With these limitations gone, the limitation will then be the inherent frequency response of the electronics of the calorimeter itself. Even though the original design never contemplated transient measurements, as it stands, the response time is better than a fraction of a minute, and so without improvements in the electronics, measurements as close to the EOB as this will be possible with a rabbit system to deliver and automatically load the samples.

It is also intended that there be extensive calculations, using existing transport codes, to accompany these measurements

ACKNOWLEDGEMENTS

We are pleased to acknowledge the help of the BLIP staff, Dr. L. Mausner, H. Schnakenberg, S. Kurczak, and D. Hunter, and also our colleague Dr. N. Tsoupas.

REFERENCES

1. C. T. Roche et al., "SMALL-SAMPLE CALORIMETER: SYSTEM DESIGN AND OPERATION", ISPO-13 Rev., April, 1981.

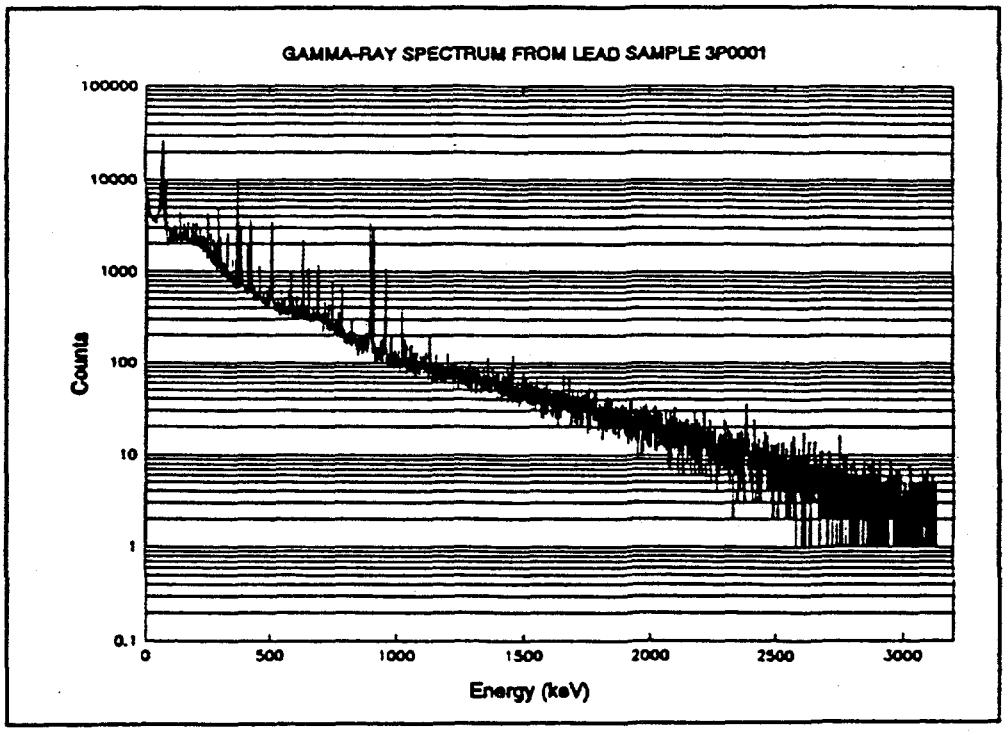

Figure 1. Gamma-ray spectrum of lead irradiated with 1-Gev protons.

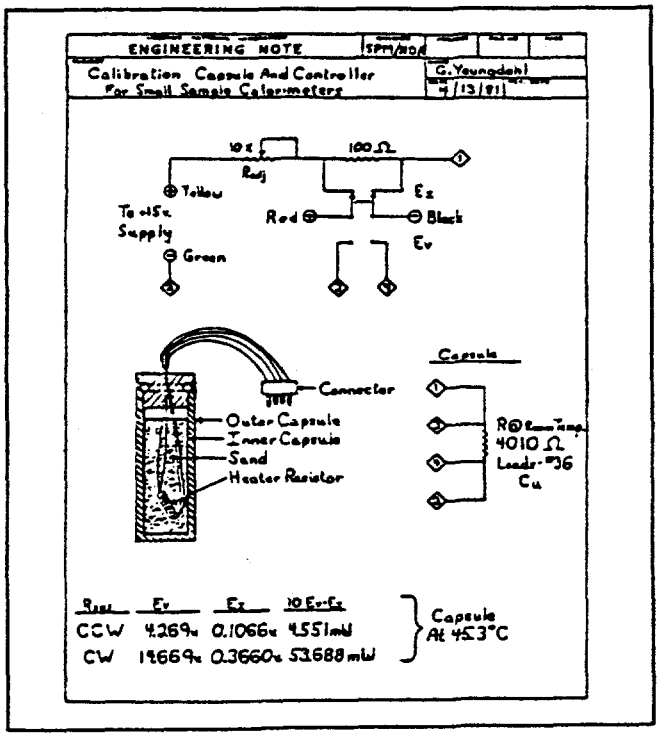

Figure 2. Electrically heated capsule.

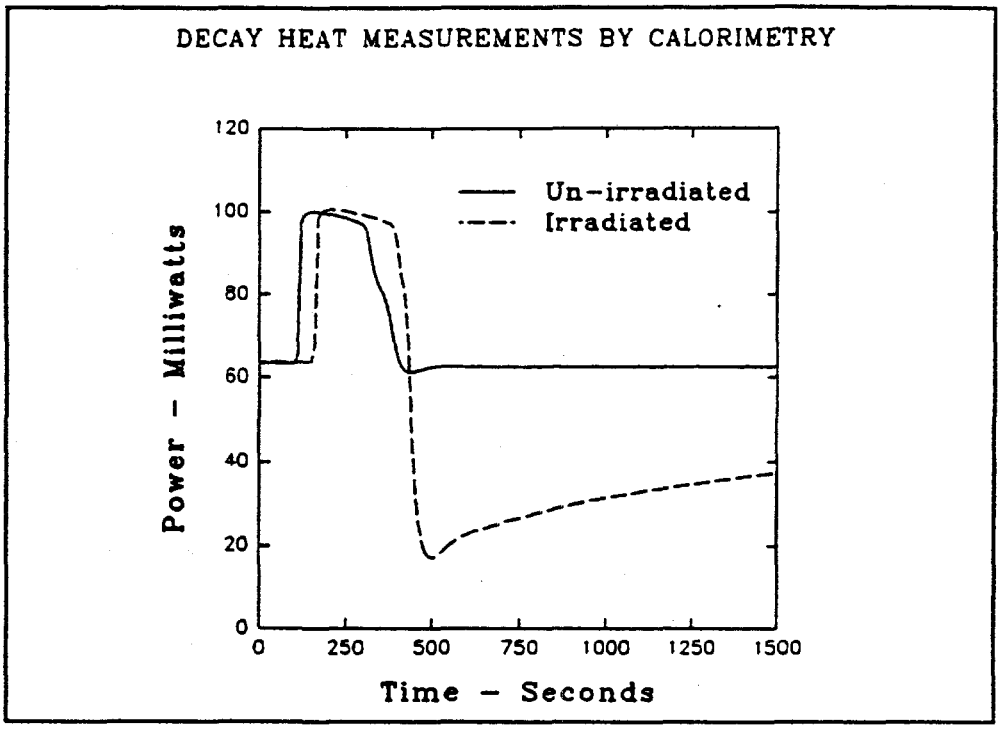

Figure 3. **Irradiated lead sample compared with un-irradiated sample.**

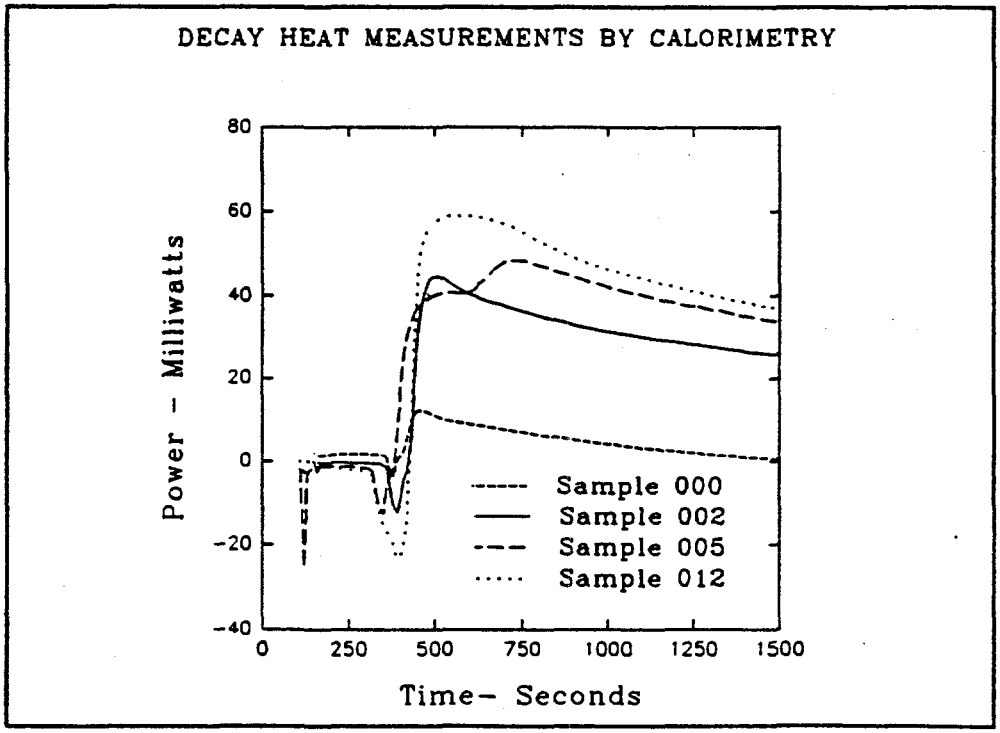

Figure 4. **Irradiated lead samples with base line subtracted.**

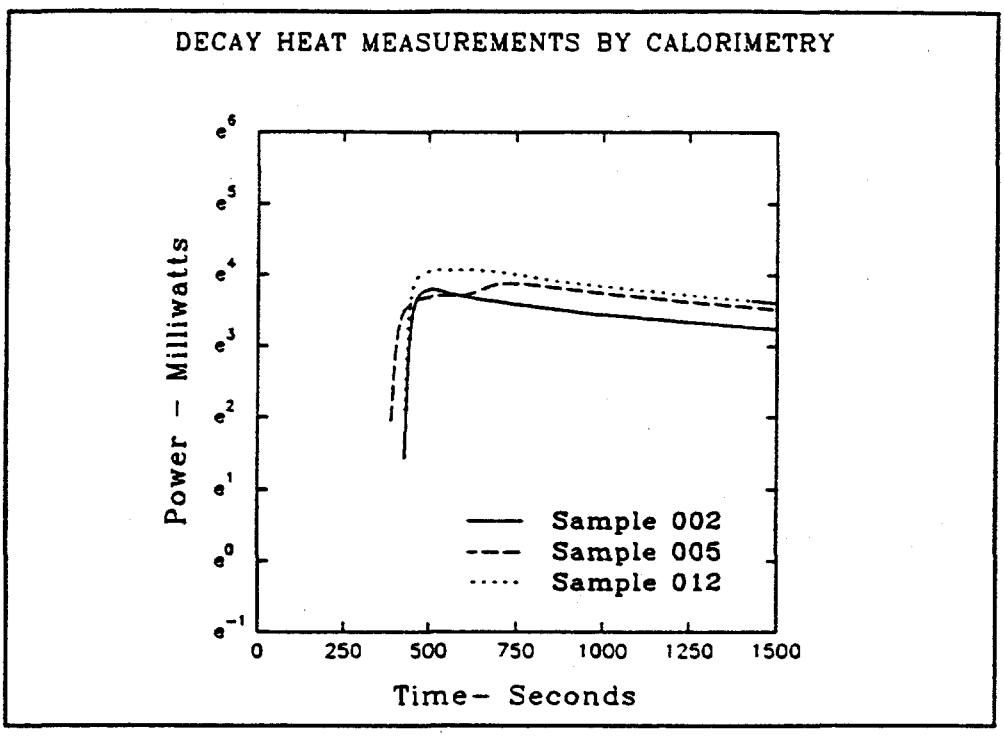

Figure 5. Irradiated lead samples with base line subtracted compared on natural log scale.

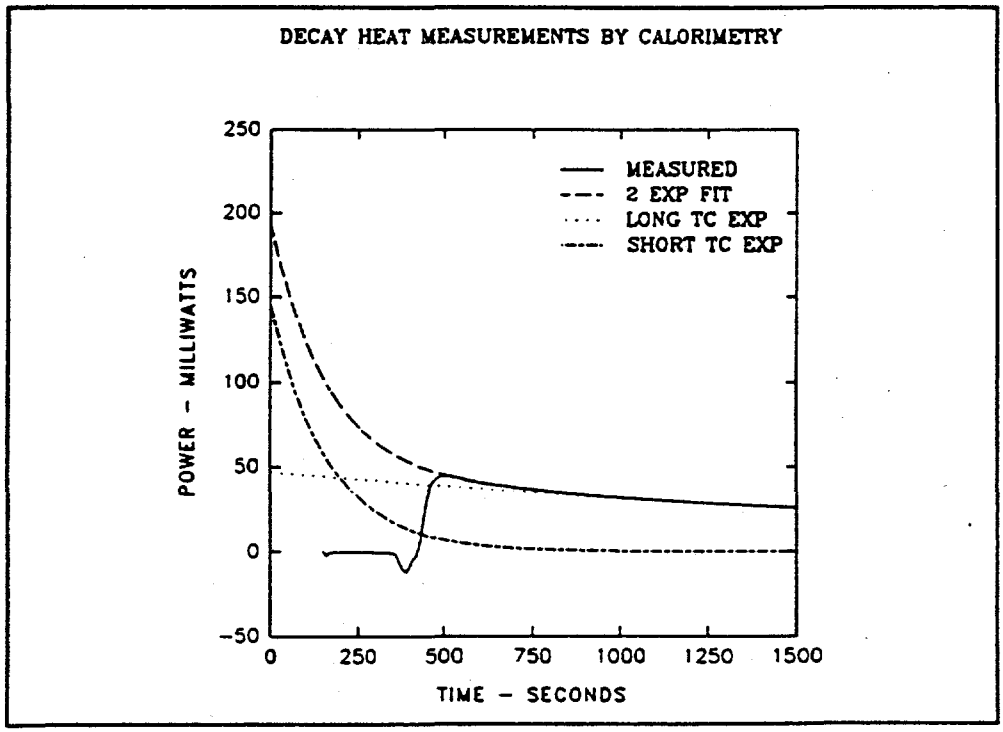

Figure 6. Irradiated lead sample 002 with base line subtracted fitted to exponential function.

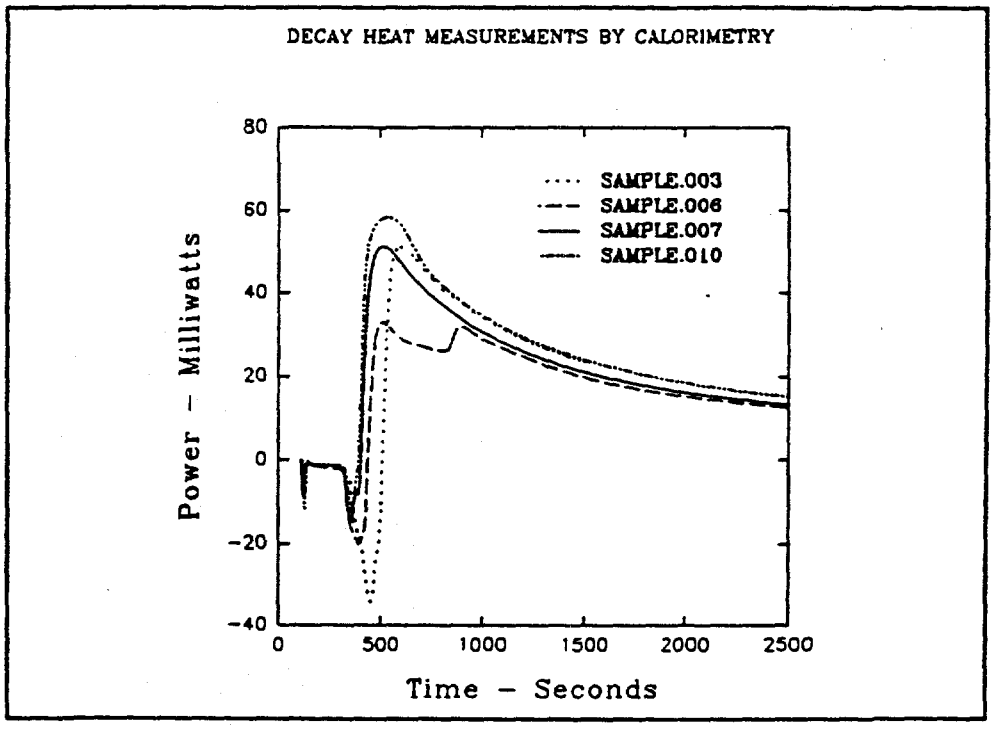

Figure 7. Irradiated tungsten samples with base line subtracted.

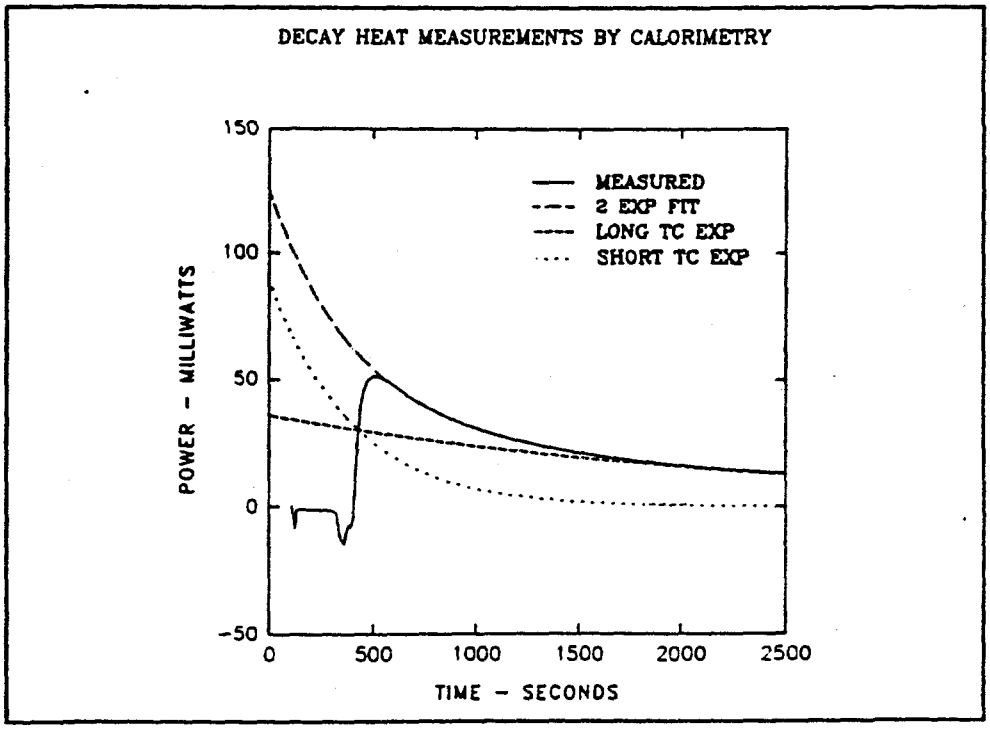

Figure 8. Irradiated tungsten sample 007 with base line subtracted fitted to exponential function.

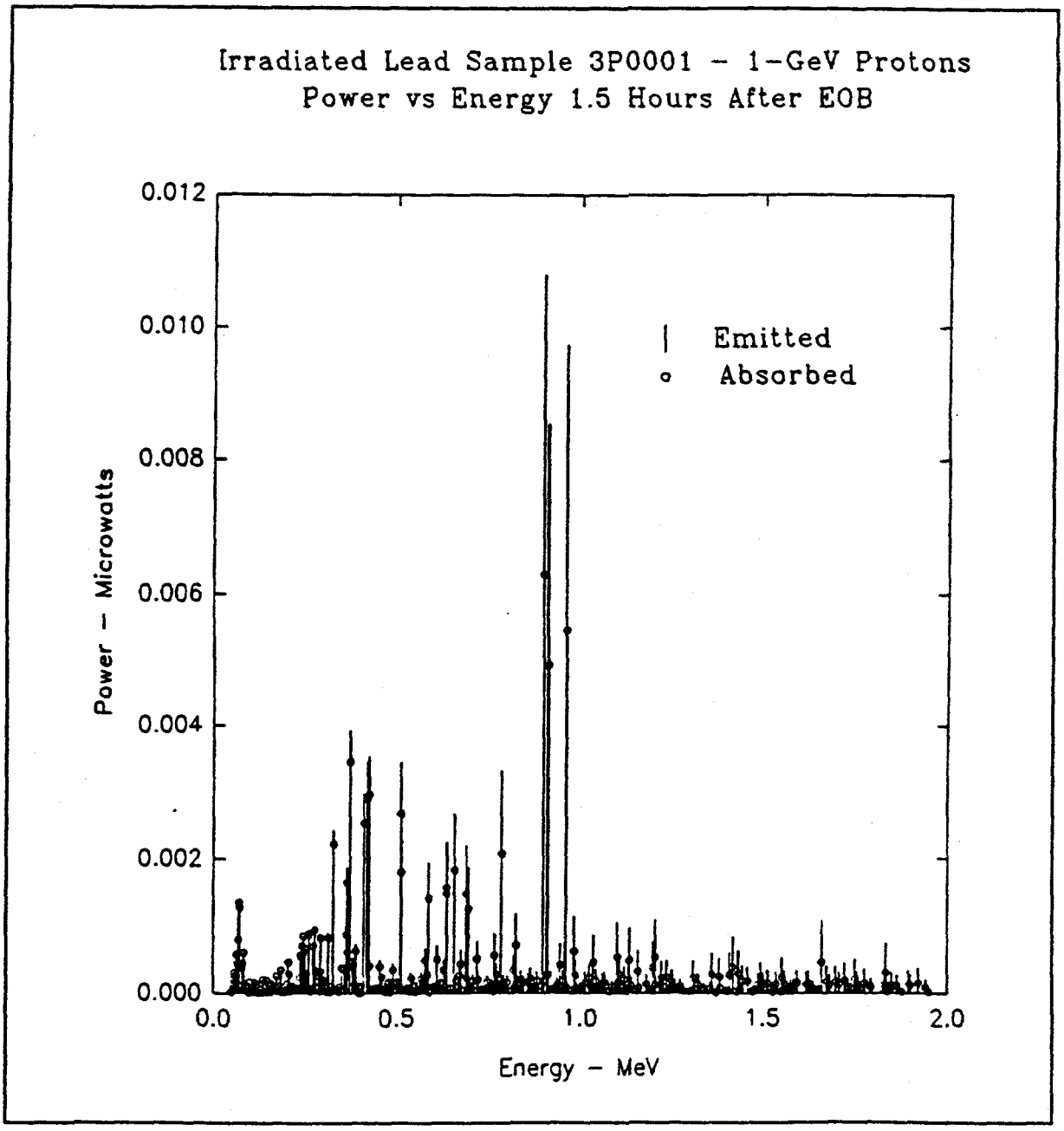

Figure 9. Power available from spectrum of sample 3P0001 to produce heat due to gamma-ray absorption.